SERS activity of photoreduced silver chloride crystals

Cite as: AIP Conference Proceedings **2220**, 050004 (2020); https://doi.org/10.1063/5.0001101
Published Online: 05 May 2020

Arpan Dutta, Antti Matikainen, Sampson Andoh, and Tarmo Nuutinen

SERS Activity of Photoreduced Silver Chloride Crystals

Arpan Dutta[1, a)], Antti Matikainen[2], Sampson Andoh[3] and Tarmo Nuutinen[3, 4]

[1]*Nanoscience Center and Department of Physics, University of Jyväskylä, Jyväskylä 40014, Finland*
[2]*Department of Electronics and Nanoengineering, Aalto University, Espoo 02150, Finland*
[3]*Institute of Photonics, University of Eastern Finland (UEF), Joensuu 80101, Finland*
[4]*Department of Environmental and Biological Sciences, UEF, Joensuu 80101, Finland*

[a)]Corresponding author: arpan.a.dutta@jyu.fi

Abstract. Metal nanoparticles are widely acclaimed as plasmonic substrates for surface-enhanced Raman spectroscopy (SERS) due to their unique particle plasmon resonances at visible and near infrared regions. Silver nanoparticles are typically employed in SERS when the targeted Raman signature zone of analytes lies at ultra-violet and/or blue to green spectral regimes. Even though silver has strong plasmonic properties, silver-based substrates are often affected by the atmospheric oxidation and show degradation in their SERS performance. One way to overcome this limitation is to use silver chloride crystals as oxidation resistant intermediate and photoreduce them to 'fresh' silver just before SERS analysis. In this work, we study the SERS activity of the photoreduced silver chloride crystals. We perform Raman analysis of three Raman active analytes, adenine, rhodamine 6G and riboflavin at both visible (514 nm) and near-infrared (785 nm) excitations. Our experimental outcomes show that such photoreduced silver chloride crystals can be exploited as SERS active substrates for both visible and near-infrared applications. Our numerical simulations reveal that these photoreduced silver chloride crystals are strong scatterers at multiple wavelengths and hence, could be very useful for plasmon-enhanced spectroscopic applications where multiple wavelengths are involved.

INTRODUCTION

Surface-enhanced Raman spectroscopy (SERS) is a modified version of normal Raman spectroscopy and it involves a plasmonic substrate to intensify the weak Raman responses of the probed material [1-3]. SERS has become a well-established analytical technique [1] and a popular method in bio-sensing [4-6] as well as in single molecule detection [7-10]. Nanoparticles, made of noble metals like silver (Ag) and gold (Au), are widely used as the plasmonic substrates in SERS due to the presence of their unique localized surface plasmon resonance (LSPR) at the visible and near-infrared (NIR) regions [11-13]. The LSPR of the particles can also be tuned to the intended spectral regions by modifying their shape, size and surface distribution [11-14].

SERS active substrates most often involve Ag for its strong plasmonic resonances in the visible range. However, application of Ag in SERS has a major challenge. In our previous work, we have shown how Ag oxidizes fast in atmospheric condition and consequently, loses its SERS activity significantly [15]. We reported that such atmospheric oxidation of Ag causes poor reproducibility and low stability in Ag based SERS substrates [15]. We also proposed an alternative solution of the aforementioned problem in our earlier work [16] by 'growing' silver chloride (AgCl) crystals on a silicon wafer and on the tip of a fiber to utilize them as an oxidation resistant intermediate which are photoreduced to 'fresh' silver just before the Raman experiments.

In this work, we report the SERS activity of the photoreduced AgCl crystals for two different excitation schemes. Our experimental outcomes show that such photoreduced AgCl crystals can be used for both visible and near infrared SERS applications. Our numerical findings also imply the possibilities of utilizing such photoreduced AgCl crystals in certain spectroscopic applications where multi-wavelength excitation scheme is involved since the photoreduced AgCl crystals are strong scatterers at multiple wavelengths.

3rd International Conference on Condensed Matter and Applied Physics (ICC-2019)
AIP Conf. Proc. 2220, 050004-1–050004-6; https://doi.org/10.1063/5.0001101
Published by AIP Publishing. 978-0-7354-1976-6/$30.00

RESULTS AND DISCUSSION

AgCl crystals were directly 'grown' onto a silicon (Si) wafer with the help of a liquid phase deposition method [16] at room temperature under standard lighting and humidity. The motivation of this synthesis method was to utilize AgCl crystals as oxidation resistant intermediate and photoreduce them for SERS just before the Raman experiments. The AgCl nanocrystals were turned into irregular shaped Ag nanoparticles (Fig. 1) after photoreduction and we studied their SERS performance with the help of three Raman active analytes, adenine (Ade), rhodamine 6G (Rh6G) and riboflavin (RFN), both at visible (514 nm) and near-infrared (785 nm) excitation conditions. The synthesis and photoreduction of AgCl crystals are briefed in *Materials and Methods* and more details can be found in our previous work [16].

Raman analysis of the chosen analytes was carried out on top of the photoreduced AgCl crystals, which are actually freshly 'grown' irregular shaped Ag nanoparticles (Fig. 1). The concentrations of the analytes and the experimental details are reported in *Materials and Methods*. Recorded SERS intensities (counts) of the analytes are presented in Fig. 2 to Fig. 4 where blue and red curves in each figure depict SERS spectrum with excitation at 514 nm and 785 nm, respectively. Figure 2 illustrates the symmetric ring-breathing mode of Ade around 734 cm^{-1} [17] while Fig. 3 resolves the N – H in-plane bend mode (around 1311 cm^{-1} and 1575 cm^{-1}) and the C – C vibrational stretching (around 1509 cm^{-1} and 1650 cm^{-1}) of Rh6G [18] for both excitation schemes. Figure 4 yields seven distinguishable SERS bands of RFN at both excitations similar with existing literature [19].

The experimental results clearly show that SERS responses at visible and at near-infrared excitations are comparable (in terms of intensity) for all analytes. Accordingly, we can conclude that the photoreduced AgCl crystals (which are irregular shaped Ag nanoparticles) are efficient enough as a plasmonic substrate for SERS applications both at visible and NIR regions since they yielded spectroscopically resolvable Raman information of all analytes in identical experimental environment for both excitation regions with acceptable signal strength. However, no concrete conclusion can be made about the trend in their SERS activity based on the excitation regimes i.e. whether they provide stronger SERS when excited at NIR or at visible wavelengths.

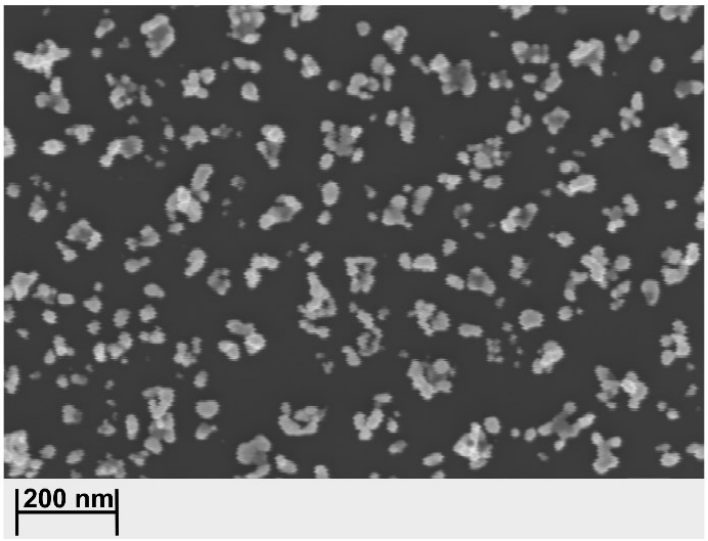

FIGURE 1. Scanning electron microscope (SEM) image of the photoreduced AgCl crystals

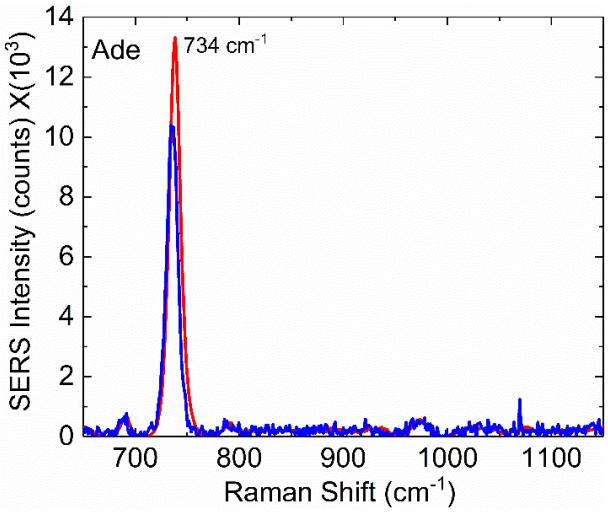

FIGURE 2. SERS spectra of Ade for excitation at 514 nm (blue curve) and 785 nm (red curve)

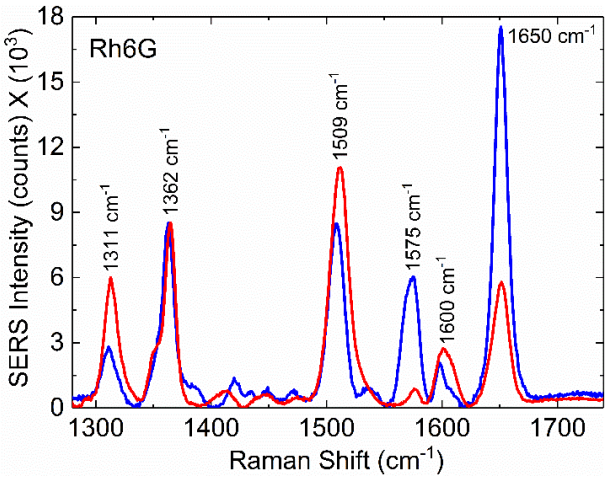

FIGURE 3. SERS spectra of Rh6G for excitation at 514 nm (blue curve) and 785 nm (red curve)

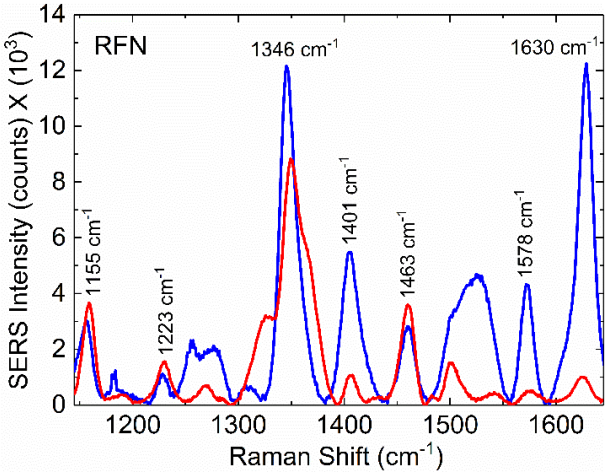

FIGURE 4. SERS spectra of RFN for excitation at 514 nm (blue curve) and 785 nm (red curve)

To investigate the underlying physical reason behind such SERS activity of the photoreduced AgCl crystals, scattering profile of a single crystal was calculated numerically with the help of an open source Mie scattering simulator MiePlot v4614. A highly simplistic geometrical model for a single photoreduced AgCl crystal was approximated from SEM image (Fig. 1) as a large solid sphere with an effective diameter of 350 nm. For more details on the computational environment, please see *Materials and Methods*.

The simulated scattering (cross-section) profile of a single photoreduced AgCl crystal, normalized by its geometrical cross-section, is presented in Fig. 5. From the figure, we can reach at a hand waving argument that the photoreduced crystals has high scattering nature in the Stoke's signal windows of analytes (700-1700 cm^{-1} i.e. 533-564 nm for 514 nm excitation and 830-906 nm for 785 nm excitation), which explains their efficient SERS activity for both excitation schemes.

MATERIALS AND METHODS

AgCl crystals were directly 'grown' onto a polished silicon (Si) wafer having approximate dimension of 0.25 × 5 × 50 mm^3 by a liquid phase deposition method [16]. In the chemical synthesis, the Si wafer was immersed in turns into 500 ml precursor solutions of 5 mM sodium chloride (NaCl) and 5 mM silver nitrate ($AgNO_3$), repetitively for 150 cycles (where the duration of one cycle was 1.5 s) to 'grow' the insoluble AgCl crystals. Consequently, the nucleation of insoluble AgCl crystals was obtained on the immersed surface of the Si wafer.

A commercially available Raman setup (inVia Raman microscope) was used for the photoactivation process and Raman measurements. The AgCl crystals were photoreduced producing irregular shaped Ag nanoparticles (Fig. 1) just before the Raman analysis by applying high intensity laser light (514 nm) on them with a radiation power of 5 mW and 10 minutes exposure time. The laser light was applied through a 20X objective (NA = 0.4) which yielded final spot size of the laser beam as 20 µm on the sample. After that, the analytes were evenly distributed on the sample surface (i.e. the photoreduced spots). The concentrations of the analytes in liquid solutions were 1 mM for Ade, 1 µM for Rh6G and 9.5 µg/l for RFN. The droplet size (5 µl) and the incubation time (5 min) were same for all analytes. For the SERS measurements at 514 nm excitation, 15.5 µW laser power was used through a 20X objective (NA = 0.4) and the accumulation time was 10 s. The incident laser beam had an approximated spot size of 20 µm on the sample. For the measurements with 785 nm excitation, all parameters were same as above except the laser power, which was 3.61 mW.

To approximate the shape and size of a photoreduced AgCl crystal for numerical simulations, SEM image of a parallel sample was captured with the help of SEMleo1550Gemini microscope operated at an accelerated voltage of 5 kV. In the computation, a single photoreduced AgCl crystal was considered as a solid Ag sphere with an effective diameter of 350 nm, surrounded by air everywhere. The scattering response at the far field for the unpolarized plane wave excitation was calculated using MiePlot v4614 (http://www.philiplaven.com/mieplot.htm). The dispersive dielectric function of silver was extracted from the reported data of Johnson and Christy [20]. The nondispersive refractive index of air was considered as 1.

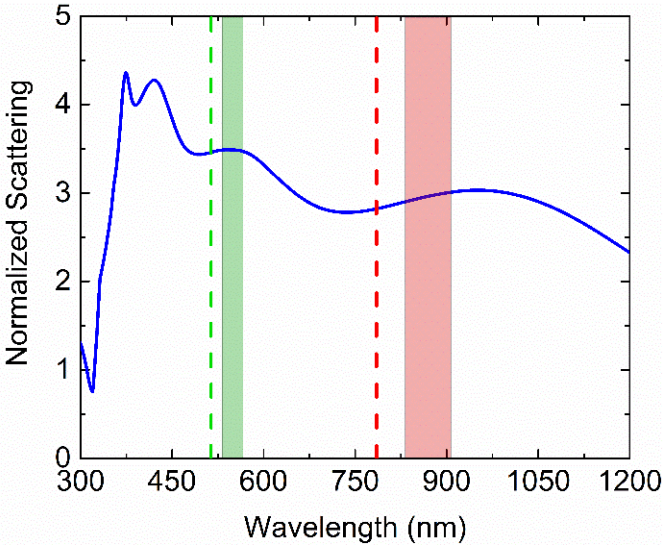

FIGURE 5. Simulated normalized scattering profile of a single photoreduced AgCl crystal in air. The green and red dotted lines (vertical) show the excitation wavelengths, 514 nm and 785 nm, respectively. The green and red shaded regions indicate the Stoke's signal window of the analytes (i.e. 700-1700 cm^{-1}), 533-564 nm (for 514 nm excitation) and 830-906 nm (for 785 nm excitation), respectively.

CONCLUSIONS

Concisely, we performed chemical synthesis of AgCl crystals by 'growing' them on top of a Si wafer and photoreduced them by laser excitation just before the SERS measurements. Our Raman analysis of Ade, Rh6G and RFN resulted in comparable SERS responses at visible and NIR excitations for each analyte. Our numerical calculation on the scattering profile of the photoreduced AgCl crystal revealed that the crystal has scattering maxima at Stoke's signal windows of analytes for both excitations and consequently, provided a hand waving explanation of our experimental findings. Our results clearly show that these photoreduced AgCl crystals can be exploited as an efficient plasmonic substrate for visible and near infrared SERS applications. Our findings also imply the possibilities of utilizing such photoreduced crystals in multi-wavelength excitation-based spectroscopic applications since the crystals provide strong scattering over a broad range of wavelengths.

ACKNOWLEDGMENTS

The authors gratefully acknowledge Assoc. Prof. Erik M. Vartiainen (LUT University, Lappeenranta, Finland) and Assoc. Prof. J. Jussi Toppari (University of Jyväskylä, Jyväskylä, Finland) for their valuable guidance during the research work.

REFERENCES

1. R. Panneerselvam, G. K. Liu, Y. H. Wang, J. Y. Liu, S. Y. Ding, J. F. Li, D. Y. Wu and Z. Q. Tian, Chem. Commun. **54**, 10-25 (2018).
2. S. Schlücker, Angew. Chem. Int. Ed. **53**, 4756-4795 (2014).
3. B. Sharma, R. R. Frontiera, A. I. Henry, E. Ringe and R. P. Van Duyne, Mater. Today **15**, 16-25 (2012).
4. A. I. Henry, B. Sharma, M. F. Cardinal, D. Kurouski and R. P. Van Duyne, Anal. Chem. **88**, 6638-6647 (2016).
5. R. A. Tripp, R. A. Dluhy and Y. Zhao, Nano Today **3**, 31-37 (2008).
6. K. C. Bantz, A. F. Meyer, N. J. Wittenberg, H. Im, Ö. Kurtulus, S. H. Lee, N. C. Lindquist, S. H. Oh and C. L. Haynes, Phys. Chem. Chem. Phys. **13**, 11551-11567 (2011).
7. E. C. Le Ru and P. G. Etchegoin, Annu. Rev. Phys. Chem. **63**, 65-87 (2012).
8. Y. Wang and J. Irudayaraj, Phil. Trans. R Soc. B **368:20120026**, 1-10 (2013).

9. H. M. Lee, S. M. Jin, H. M. Kim and Y. D. Suh, Phys. Chem. Chem. Phys. **15**, 5276-5287 (2013).
10. A. B. Zrimsek, N. Chiang, M. Mattei, S. Zaleski, M. O. McAnally, C. T. Chapman, A. I. Henry, G. C. Schatz and R. P. Van Duyne, Chem. Rev. **117**, 7583-7613 (2017).
11. W. Li, X. Zhao, Z. Yi, A. M. Glushenkov and L. Kong, Anal. Chim. Acta **984**, 19-41 (2017).
12. S. A. Maier, *Plasmonics: Fundamentals and Applications* (Springer, Berlin, 2007), pp. 65-88.
13. M. Pelton and G. W. Bryant, *Introduction to Metal-Nanoparticle Plasmonics* (Wiley, New Jersey, 2013), pp. 1-46.
14. Y. Xia and N. J. Halas, MRS Bull. **30**, 338-343 (2005).
15. A. Matikainen, T. Nuutinen, T. Itkonen, S. Heinilehto, J. Puustinen, J. Hiltunen, J. Lappalainen, P. Karioja and P. Vahimaa, Sci. Rep. **6**, 37192 (2016).
16. A. Matikainen, T. Nuutinen, P. Vahimaa and S. Honkanen, Sci. Rep. **5**, 8320 (2015).
17. F. Madzharova, Z. Heiner, M. Gühlke and J. Kneipp, J. Phys. Chem. C **120**, 15415-15423 (2016).
18. C. Wu, E. Chen and J. Wei, Colloids Surf. A: Physicochem. Eng. Aspects **506**, 450-456 (2016).
19. M. Švecová, P. Ulbrich, M. Dendisová and P. Matějka, Spectrochim. Acta A **195**, 236–245 (2018).
20. P. B. Johnson and R. W. Christy, Phys. Rev. B **6**, 4370-4379 (1972).